

Radio Frequency Signature Correlation Based Speed Estimation for Indoor Positioning

Mostafa Afgani, Sinan Sinanović, Karim Khashaba*, Harald Haas

Institute for Digital Communications, School of Engineering & Electronics, The University of Edinburgh, UK

*School of Engineering & Science, Jacobs University Bremen, Germany

Email: h.haas@ed.ac.uk

Abstract—Dead reckoning represents a class of methods for relative position estimation based on a previously determined absolute reference position. The estimate is formulated from a combination of the known speed, time and heading information with the known reference position. One of the main obstacles to effective positioning of pedestrians via dead reckoning is the lack of accurate speed estimation algorithms. Existing methods are either complex or provide results that are unsatisfactory at the low velocities associated with pedestrians. In contrast, the two algorithms proposed in this paper are relatively simple to implement and provide accurate results at low velocities. In the first algorithm, a one-dimensional and unidirectional two-antenna solution is described where the speed can be easily estimated from a knowledge of the fixed inter-antenna distance and the time it takes for the trailing antenna to sense the same channel conditions (radio frequency (RF) signature) previously observed at the leading antenna. Computer simulations show that, with typical estimation errors of less than 2.67% around average pedestrian speeds, the approach is indeed effective and accurate. A by-product of the algorithm is an environment specific spatial correlation function which is used in the second algorithm to provide even better estimates. With the improvements offered by the latter algorithm, relative errors of merely around 0.15% on average are achievable. This improvement in performance over the first algorithm comes at the cost of slightly higher computational complexity. When subsequently used for user displacement estimation, a relatively small error of 24.5cm is observed after a duration of 60s.

Index Terms—speed estimation, pedestrian dead reckoning, spatial correlation, radio frequency signature matching

I. INTRODUCTION

Pedestrian dead reckoning (PDR) is a popular choice for positioning and navigation in areas (e.g. indoors) where Global Positioning System (GPS) based solutions cannot be used. Two pieces of information are essential before a valid location estimation can be made: a reference point with known coordinates and the velocity (speed and heading) at sufficiently close and successive intervals. Given the needed information, displacement of

This paper is based on “Speed Estimation Using Relative Radio Frequency Signature Matching,” by M. Afgani, and H. Haas, which appeared in the Proceedings of the 66th IEEE Vehicular Technology Conference (VTC), Baltimore, USA, September/October 2007. © 2007 IEEE.

This research was conducted in cooperation with MobilTec GmbH as part of the Mobile Positioning System (MPos) project, funded by the BIS (Bremerhavener Gesellschaft für Innovationsförderung und Stadtentwicklung mbH) within the T.I.M.E. program (grant 56023/2 VN) of the State of Bremen/Bremerhaven, Germany.

the user from the reference location can be approximated and, hence, an estimate of the new location coordinates can be obtained.

Accurate heading information is readily available from sensors such as a ring laser gyro [1]; it is the speed estimate that has been difficult to obtain with a sufficient degree of accuracy. Step length estimation based devices ([2], [3]) can only be used by pedestrians and must be mounted directly on the person. Frequent updates of the absolute position are also required as errors tend to accumulate with every step. While methods based on the level crossing rate (LCR) of the received Rayleigh fading envelope ([4], [5]) typically provide good results for high speeds, the accuracy drops considerably at speeds associated with pedestrians and other low velocity entities. Continuous wavelet transform (CWT) can also be used to extract speed information from the aforementioned envelope with a good degree of accuracy [6], however such a procedure is computationally complex and expensive.

In this paper, two novel methods of speed estimation are described. The first proposed method, termed relative radio frequency signature matching (RRFSM), correlates the RF signatures at two antennae separated by a known distance to determine the time it takes for the trailing antenna to experience the same channel conditions as that previously experienced by the leading antenna. As the antenna separation is predefined and known (e.g. in a MIMO (multiple-input-multiple-output) device), the speed is easily calculated from an estimate of the time delay. As will be shown later, the new speed estimation approach also employs an adaptive algorithm that allows accurate estimates at both high and low velocities. Furthermore, it is of low computational complexity as the main operation only involves the calculation of correlation values between two channel estimates which are based on the known existing radio frequency transmission in the environment.

The second algorithm uses the first to compute a spatial correlation function. Then, based on this knowledge, the correlation of the channel data at two different locations can be used to estimate the speed. This refinement, while adding some complexity to the speed estimation, is capable of lowering the estimation errors.

The rest of this paper is organised as follows. In Section II the wireless channel model considered is presented and in Section III speed estimation algorithms are

described. Section IV provides details of the realisation and the simulation results. Section V concludes the paper.

II. WIRELESS CHANNEL MODEL

The multipath effect is a common phenomenon in typical terrestrial environments. The RMS (root mean square) delay spread of the power delay profile determines the coherence bandwidth of the channel. In future broadband wireless communications, the coherence bandwidth is typically smaller than the total channel bandwidth which results in frequency selective fading. In addition to frequency selective fading, signal frequencies can also experience spreading (frequency dispersion) caused by Doppler shifts. For antenna arrays, the impulse response vector $\mathbf{h}(t)$ of a multipath channel can be represented by

$$\mathbf{h}(t) = \sum_{l=0}^{L(t)-1} A_l(t) e^{j\phi_l(t)} \mathbf{a}(\theta_l(t)) \delta(t - \tau_l(t)) \quad (1)$$

where $L(t)$ is the number of multipath components, A_l is the amplitude, ϕ_l is the carrier phase shift, θ_l is the angle of arrival (AoA) of the l^{th} multipath component, $\delta(\cdot)$ is the unit impulse function and τ_l is the time delay of the l^{th} multipath component. $\mathbf{a}(\theta_l(t))$ is known as the array response vector. When the signal and the antenna array (containing m antennae) at the receiver are restricted to a two-dimensional (2D) space, the array response vector is given by

$$\mathbf{a}(\theta_l(t)) = \begin{bmatrix} \exp(-j\Psi_{l,1}) \\ \exp(-j\Psi_{l,2}) \\ \exp(-j\Psi_{l,3}) \\ \dots \\ \exp(-j\Psi_{l,m}) \end{bmatrix} \quad (2)$$

where $\Psi_{l,i}(t) = [x_i \cos(\theta_l(t)) + y_i \sin(\theta_l(t))] \beta$. The spatial coordinate pair (x_i, y_i) represents the location of the antenna element i in 2D space. $\beta = \frac{2\pi}{\lambda}$ is the wavenumber [7], with λ being the carrier wavelength.

For line-of-sight (LoS) channels, the amplitude can be modeled by a Rician random variable, with the Rician parameter representing the relative strength of the LoS component. A Rayleigh distributed random variable is used instead when there is no single dominant multipath component. The phase shift is often assumed to be uniformly distributed within the interval $[0, 2\pi]$. The AoA is highly dependent on the relative geometry of the environment and the heights of the scatterers and the receiver. Although the assumption that the AoA is uniformly distributed within the interval $[0, 2\pi]$ is valid under certain circumstances, there are other models that are more suitable for a given channel model. An overview is provided in [7]. The delay associated with each multipath component is generally assumed to be exponentially distributed [8].

The maximum Doppler shift, $f_{d(\text{max})}$, experienced by a receiver is dependent on the speed, v , and is given by [9]:

$$f_{d(\text{max})} = \frac{v}{\lambda}. \quad (3)$$

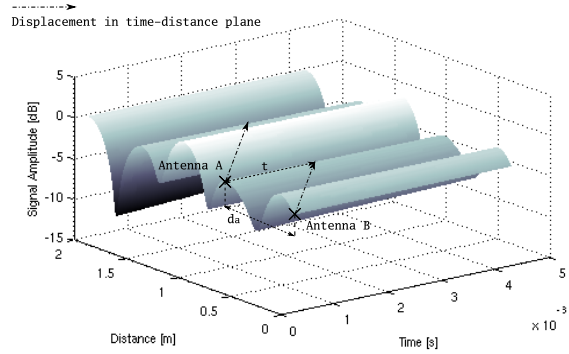


Fig. 1. Multipath channel in time and space simulated for a carrier frequency of 474MHz (DVB-T) and a speed of 1.5ms^{-1} . Assuming that the movement is restricted to the single direction parallel to the antenna array A-B, after t seconds *antenna B* is where *antenna A* was and experiences the same channel response that *antenna A* experienced t seconds ago. As the distance, d_a , between the antennae is known, the speed is easily estimated as $|v| = \frac{d_a}{t}$.

The presence of Doppler spread in a multipath channel causes it to display variations in time: the higher the Doppler frequency, the shorter is the coherence time [9],

$$T_c = \frac{0.423}{f_{d(\text{max})}}, \quad (4)$$

of the channel. The terrestrial digital video broadcast (DVB-T) service is ubiquitous and wideband – allowing the frequency selective nature of the channel to be captured over a wide range of locations. Each channel is 8MHz wide and the first has a carrier frequency of 474MHz [10]. A DVB-T receiver travelling at a typical pedestrian velocity of approximately 1.5ms^{-1} experiences a rather insignificant maximum Doppler frequency of 1.6Hz and hence a relatively long channel coherence time of 0.26s. Fig. 1 shows the space-time characteristics of a multipath Rayleigh fading channel as experienced by such a receiver.

It is clear from the plot that although the channel stays relatively unchanged over the duration of the coherence time, it shows rapid variations in space. The spatial correlation, $\rho(d, \theta)$, between signal envelopes separated by a distance d , along some azimuthal direction θ is approximated by

$$\rho(d, \theta) \approx \exp \left[-23\Lambda^2 (1 + \gamma \cos[2(\theta - \theta_{\text{max}})]) \left(\frac{d}{\lambda} \right)^2 \right] \quad (5)$$

as derived in [11]. Λ is the angular spread defined as

$$\Lambda = \sqrt{1 - \frac{|F_1|^2}{F_0^2}}, \quad (6)$$

γ is the angular constriction defined as

$$\gamma = \frac{|F_0 F_2 - F_1^2|}{F_0^2 - |F_1|^2}, \quad (7)$$

θ_{max} is the azimuthal direction of maximum fading defined as

$$\theta_{\text{max}} = \frac{1}{2} \arg(F_0 F_2 - F_1^2), \quad (8)$$

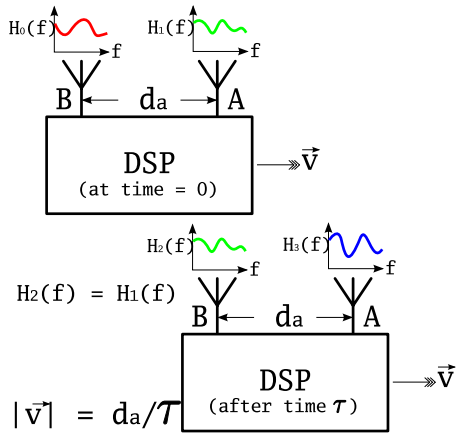


Fig. 2. Speed estimation using relative RF signature matching. The time τ required by the device to traverse the fixed distance d_a can be estimated by correlating the channel responses obtained at the two antennae. From an estimate of τ , the speed $|v|$ is easily calculated using $|v| = \frac{d_a}{\tau}$.

and F_n is the n^{th} complex Fourier coefficient of the angular distribution of multipath power (ADP), $p(\theta)$:

$$F_n = \int_0^{2\pi} p(\theta_x) \exp(jn\theta_x) d\theta_x. \quad (9)$$

As stated earlier, temporal variations in the channel are quantified by a measure of the coherence time, T_c . A similar measure of the spatial channel variations can be developed using (5). If the coherence distance, D_c , is defined as the distance at which the spatial correlation coefficient drops to 0.5, i.e. $\rho(D_c) = 0.5$, it can be approximated by [11]

$$D_c \approx \frac{\lambda \sqrt{\ln 2}}{\Lambda \sqrt{23 (1 + \gamma \cos [2(\theta - \theta_{\max})])}}. \quad (10)$$

For an omnidirectional Rayleigh fading channel, the coherence distance is often approximated by [11]

$$D_c \approx \frac{9\lambda}{16\pi}. \quad (11)$$

Applying this equation to the DVB-T system mentioned earlier produces a coherence distance of approximately 11cm. This is in agreement with the spatial variations observed in Fig. 1.

III. SPEED ESTIMATION ALGORITHMS

The spatial and temporal correlation properties of a wireless channel makes it ideal for exploitation in mobile speed estimation. Given a source of RF (radio frequency) signal and a receiver equipped with multiple antennae, relative RF signature matching can be used to estimate the speed of the receiver unit. The following sections describe the algorithms that utilise the fading characteristics of the received RF signal to provide an estimate of the speed.

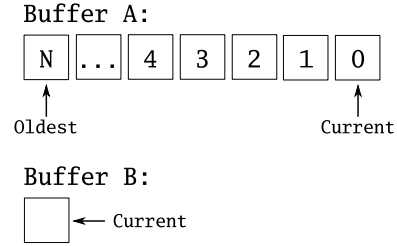


Fig. 3. Structure for the database used to store the channel response estimates.

A. Method I: Relative RF Signature Matching (RRFSM)

It is possible to estimate the speed of a MIMO mobile wireless device by comparing the channel response observed at each of the antenna array elements. The simplest such device consists of a receiver with two antennae as illustrated in Fig. 2. Motion is assumed to be restricted to a single spatial dimension and the antenna array is aligned parallel to the direction of motion. This results in a simplification of $\Psi_{l,i}(t)$ in (2) to $[x_i \cos(\theta_l(t))]\beta$.

In operation, the speed estimator traces a diagonal path in the spatio-temporal plane as illustrated in Fig. 1. Labelling the antenna array elements by the letters “A” and “B” respectively, the starting position, $(A, B)_{t_0}$, of the array elements can be denoted by the spatio-temporal coordinate pair $[(x_1, t_0), (x_0, t_0)]$. The radio channel sensed at the array elements, $(H_A, H_B)_{t_0}$, can be similarly represented by $[(H_1, t_0), (H_0, t_0)]$.

Assuming a non-zero velocity, the coordinates are $[(x_3, t_0 + \tau), (x_2, t_0 + \tau)]$ and the channel responses are $[(H_3, t_0 + \tau), (H_2, t_0 + \tau)]$ after some time τ . For some value of $\tau = \tilde{\tau}$, $x_2 = x_1$ and $H_2 \approx H_1$ due to the relatively large coherence time of the channel. This implies that the device travels a distance $d_a = x_1 - x_0$ in that time. Since d_a is the inter-antenna separation distance, it is constant and known *a priori*. Therefore, the speed of the device is easily estimated from an estimate of $\tilde{\tau}$ using

$$|\vec{v}| = \frac{d_a}{\tilde{\tau}}. \quad (12)$$

It is possible to obtain an estimate of the time delay, $\tilde{\tau}$ by comparing the channel responses observed at the antenna array elements. Accurate channel estimates or knowledge of the underlying fading process is not required as the proposed method only looks for a relative match between channel responses. This also implies that a reasonably low amount of uncertainty and errors in the estimates can be safely ignored as long as all the estimates are affected in a similar fashion.

Clearly, a history of the channel responses observed at the “leading” antenna (A in this case) must be maintained. Fig. 3 illustrates the structure of a database that stores the current and N previous channel response estimates (CREs) and associated timestamps for antenna A. The instantaneous CRE of antenna B is also stored for the duration of the signal correlation computation.

The operation used to find the the CRE leading to maximum correlation is:

$$\text{idx} = \underset{k}{\operatorname{argmax}} (B \star A_k); k = 1, \dots, N. \quad (13)$$

idx is the database index corresponding to the CRE from antenna element A yielding maximum correlation and can be used to determine the elapsed time from the associated timestamp. The binary operator “ \star ” represents cross-correlation at a lag of zero. It is unnecessary to compute $B \star A_0$ since it implies a time delay of zero and hence infinite speed.

The cross-correlation of two signals at a lag of zero is identical to their *dot-product*. As a result, (13) can be simplified to a series of normalised dot-product calculations followed by maximum detection:

$$\text{idx} = \underset{k}{\operatorname{argmax}} \left(\frac{B \cdot A_k}{\|B\| \cdot \|A_k\|} \right); k = 1, \dots, N. \quad (14)$$

The range of speeds detectable with such a device ultimately depends on the estimation rate and the CRE history buffer maintained. With v_{\min} and v_{\max} as bounds to the detectable speed range, the time delay between CRE estimates must be less than $\frac{d_a}{v_{\max}}$ for some inter-antenna separation distance d_a . On the other hand, correct estimation of v_{\min} requires the ability to store CRE estimates spanning a time of at least $\frac{d_a}{v_{\min}}$. Assuming that the CRE estimation interval is short enough to detect v_{\max} , the total number of past CREs to store are:

$$N = \left\lceil \frac{\left(\frac{d_a}{v_{\min}} \right)}{\left(\frac{d_a}{v_{\max}} \right)} \right\rceil = \left\lceil \frac{v_{\max}}{v_{\min}} \right\rceil. \quad (15)$$

Since the time delay is estimated from a correlation between CREs, the instantaneous channel response must be estimated periodically. For a wireless system with symbol duration T_s , the CRE estimation interval \hat{i} can be defined as the number of complete symbols that elapse between the CRE estimates:

$$\hat{i} = \left\lfloor \frac{\alpha}{\mu} \right\rfloor, \quad (16)$$

where α is a constant defined as

$$\alpha = \frac{d_a}{v_{\max} \times T_s} \quad (17)$$

and μ is an adaptive scaling parameter. By adjusting the CRE estimation interval in accordance with the estimated speed of the device, it attempts to provide higher accuracy in the time delay estimates.

The parameter μ is a real number bounded by the constant α and 1, allowing \hat{i} to assume integer values within the range $\hat{i}_{\min} = 1$ and $\hat{i}_{\max} = \lfloor \alpha \rfloor$. A CRE estimation interval lower than \hat{i}_{\min} is impossible as it implies an interval shorter than a symbol. An interval longer than \hat{i}_{\max} is unnecessary as it would provide speed estimates lower than v_{\min} for a given value of N .

Initially, the adaptive parameter μ is set to 1 so that $\hat{i} = \hat{i}_{\max}$. This allows for a rough estimate, v_{est} , to be obtained for any speed between v_{\min} and v_{\max} . Given

that estimate, linear interpolation is employed to obtain the new value of μ and hence \hat{i} :

$$\mu = \begin{cases} m \cdot (v_{\text{est}} - v_{\min}) + 1, & v_{\min} \leq v_{\text{est}} \leq (v_{\max} + \epsilon) \\ 1, & \text{otherwise} \end{cases} \quad (18)$$

where

$$m = \frac{\alpha - 1}{v_{\max} - v_{\min}} \quad (19)$$

and ϵ is a small number required to allow the adaptive procedure to converge at the upper bound of the detectable speed range. Defining the maximum speed detectable with $\mu = 1$ as

$$\tilde{v}_{\max} = \frac{d_a}{T_s \times \hat{i}_{\max}} \quad (20)$$

and Δv_{\max} as the absolute difference between \tilde{v}_{\max} and v_{\max}

$$\Delta v_{\max} = |\tilde{v}_{\max} - v_{\max}|, \quad (21)$$

ϵ is defined as

$$\Delta v_{\max} \leq \epsilon \leq 1.1 \Delta v_{\max}. \quad (22)$$

Since only a lower bound to ϵ is logically defined, an arbitrary upper bound of $1.1 \Delta v_{\max}$ is introduced to provide a sensible limit to the possible choices of ϵ .

While the first case in (18) is useful for adapting the value of μ while the device is in motion, the second case is necessary to reset the value of μ to 1 in case of erroneous estimates (e.g. $v_{\text{est}} \gg v_{\max}$) or when the device is stationary ($v_{\text{est}} = 0$).

Due to the integer nature of \hat{i} , any time delay estimated is generally an integer multiple of T_s . As a result, the speeds estimated between v_{\min} and v_{\max} do not form a continuous range:

$$v_{\text{est}} = \frac{d_a}{k \times T_s \times \hat{i}}. \quad (23)$$

k is an integer related to the idx in (14).

Example Let $v_{\min} = 0.1\text{ms}^{-1}$, $v_{\max} = 15\text{ms}^{-1}$, $T_s = 224\mu\text{s}$, $\hat{i} = \hat{i}_{\max} = 14$, $d_a = 0.05\text{m}$, and $N = 150$. The speeds detectable are then 15.94ms^{-1} , 7.97ms^{-1} , 5.31ms^{-1} , \dots , 0.106ms^{-1} corresponding to $k = 1, 2, 3, \dots, N$ respectively.

The example cited also indicates that the performance is quite poor in the vicinity of v_{\max} with $\hat{i} = \hat{i}_{\max}$. This is due to the fact that the CRE estimation interval is not short enough to provide the time resolution needed at higher speeds. Table I compares the result of using $\hat{i} = \hat{i}_{\max}$ and $\hat{i} = \hat{i}_{\min}$ for the example provided.

The tabulated data indicates that a longer estimation interval works well for speeds in the vicinity of v_{\min} while higher speeds require shorter estimation intervals for more accurate estimates. The improved accuracy at in the vicinity of v_{\max} comes at the cost of the minimum speed detectable – it increases to 1.4881ms^{-1} when $\hat{i} = \hat{i}_{\min}$.

From (18) it is clear that the adaptive parameter μ always tries to provide the most suitable \hat{i} for a given database size – higher values of v_{est} result in higher

TABLE I
THE EFFECT OF THE CRE ESTIMATION INTERVAL ON SPEEDS
DETECTABLE.

$\hat{i} = \hat{i}_{\max} = 14$		$\hat{i} = \hat{i}_{\min} = 1$	
k	Speed (m/s)	k	Speed (m/s)
1	15.944	1	223.21
2	7.9719
3	5.3146	14	15.944
4	3.9860	15	14.881
...	...	16	13.951
148	0.10773
149	0.10701	149	1.4981
150	0.10629	150	1.4881

values of μ which in turn lead to a reduction in the CRE estimation interval. The opposite is true for lower values of v_{est} .

While it is obvious that the setting $\hat{i} = \hat{i}_{\min}$ yields the finest time resolution possible and hence the most accurate results, it is inefficient in practice as the number of past CRE estimates that must be stored in memory to detect v_{\min} is prohibitively large ($N = 4465$ for a DVB-T receiver with $T_s = 224\mu\text{s}$, $d_a = 10\text{cm}$, $v_{\min} = 0.1\text{ms}^{-1}$). Dynamically adjusting \hat{i} to the estimated speed allows the RRFSM algorithm to be more memory efficient ($N = 150$ for $v_{\min} = 0.1\text{ms}^{-1}$ and $v_{\max} = 15\text{ms}^{-1}$).

Table I also shows that with the initial value of $\hat{i} = 14$ and hence $\mu = 1$, a true speed of 15ms^{-1} is most likely to be detected as 15.944ms^{-1} . At the absence of the parameter ϵ , μ will always remain at that initial value (since the condition $v_{\text{est}} \leq (v_{\max} + \epsilon)$ in (18) would not be satisfied) and hence the speed will continue to be estimated as 15.944ms^{-1} . With $\epsilon = 1$, however, that condition will be satisfied and μ will be increased accordingly – reducing the estimation interval and yielding an estimate that is more precise than the last.

To avoid erroneous speed estimates, the maximum value produced by (14) must be above a sufficiently high threshold. If that value is below the threshold, the CREs at the antenna elements are assumed to be uncorrelated and hence the device is assumed to be at a standstill. It is important to pick a suitable threshold as a value too low may result in erroneous results while a value too high will reduce the sensitivity of the algorithm. It may be possible to determine a sensible threshold from spatial correlation models of the channel or real-world experiments.

A flow diagram of the one dimensional and uni-directional algorithm is shown in Fig. 4. The method can be extended for multi-dimensional speed estimation by intelligently combining the results from additional antenna arrays oriented parallel to each of the spatial dimensions desired.

B. Method II: Modified RRFSM

The algorithm described in Section III-A produces discrete speed estimates and as such is generally not expected to be exact. However, the method can be further

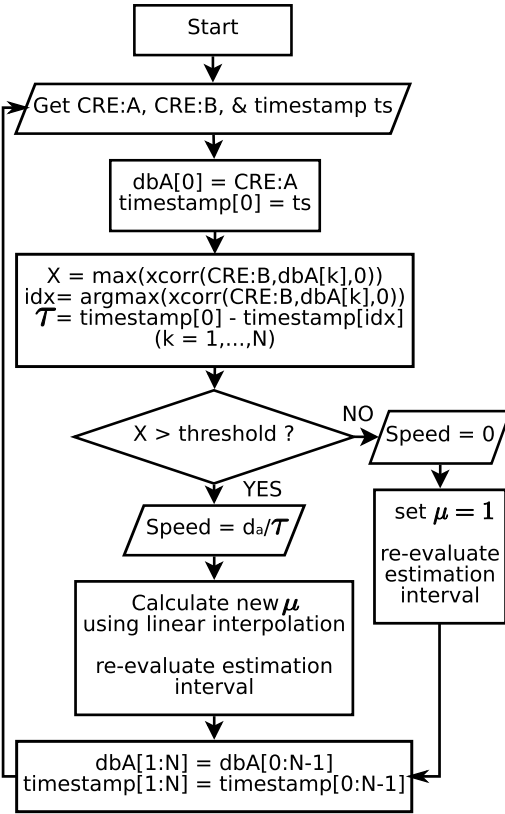


Fig. 4. 2-antenna speed estimation algorithm. “dbA[]” is the CRE buffer associated with antenna A. The function $\text{xcorr}(a, b, L)$ provides the normalised cross correlation product at delay = L (i.e. it performs the operations necessary to compute the parenthesised expression in (14)).

extended by utilising the signal spatial correlation model described by (5).

Once again, assuming that the motion of the antenna array is restricted to a single constant direction θ_0 , (5) can be simplified to:

$$\rho(d) \approx \exp \left[-23\Lambda^2 (1 + \gamma \cos [2(\theta_0 - \theta_{\max})]) \left(\frac{d}{\lambda} \right)^2 \right]. \quad (24)$$

As Λ , γ , and θ_{\max} are also constants for a given ADP (see Section II), the equation can be further simplified to:

$$\rho(d) \approx \exp \left[-23K \left(\frac{d}{\lambda} \right)^2 \right], \quad (25)$$

where the constant K is defined as

$$K = \Lambda^2 (1 + \gamma \cos [2(\theta_0 - \theta_{\max})]). \quad (26)$$

Therefore, given the inverse function of (25):

$$d \approx \lambda \sqrt{-\frac{\ln(\rho)}{23K}}, \quad (27)$$

it is possible to estimate the distance d between two signal envelopes given their correlation factor ρ , the signal wavelength λ , and the channel dependent constant K . If the time delay τ between the envelopes is known, an estimate of the speed can be obtained from the estimate

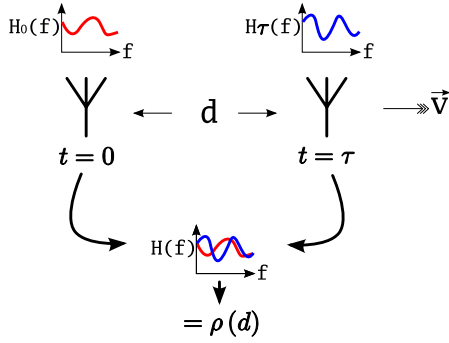


Fig. 5. Speed estimation using signal spatial correlation (modified RRFSM). Knowledge of the channel parameters and the correlation ρ between two signal fading envelopes sampled τ seconds apart allows the distance traversed to be estimated using (29). The speed, $|v|$, can then be estimated using $|v| = \frac{d}{\tau}$.

of d using (12) by substituting d for d_a . The concept is illustrated in Fig. 5. Assuming that the value of K is known, a single antenna can be used for speed estimation using (27).

Unfortunately, the parameter K is directly related to the ADP which is highly dependent on the geometry of the radio environment. Therefore it is virtually impossible to obtain an analytical expression for the instantaneous value of K . Hence it must be estimated before the speed estimation algorithm can be applied. Reordering of the variables in (27) provides an approximation

$$K \approx -\frac{\ln(\rho)}{23} \left(\frac{\lambda}{d}\right)^2 \quad (28)$$

in terms of the envelope correlation ρ and the distance d .

This is where the scheme described in Section III-A can be exploited. While evaluating (14), the CRE at antenna B is correlated against all the CREs in the database to yield a set of correlation factors $(\rho_1, \rho_2, \rho_3, \dots, \rho_N)$. Then, using the rough speed estimate, v_{est} , each correlation factor ρ_k can be mapped to a distance d_k using

$$d_k = d_a - (t_k \cdot v_{\text{est}}); \quad k = L, L + 1, \dots, M \quad (29)$$

where t_k is the time delay associated with ρ_k and L and M define a subset of the coefficients that meet some suitability criterion as explained later in this section. Given the set of correlation coefficients and their associated distance estimates, a set of estimates for K can be obtained using (28). The final estimate K' is then obtained by taking the arithmetic mean over that set:

$$K' = \frac{1}{M - L + 1} \sum_{k=L}^M K'_k. \quad (30)$$

Since K' is an estimate of the true value of K , it is necessary to evaluate its accuracy. Given the procedure employed to obtain the estimate, the most likely source of errors are the correlation coefficients ρ_k and v_{est} . As v_{est} already represents the “best-effort” of the algorithm in Section III-A, an attempt is made to pick the most suitable set of correlation coefficients. The relative error

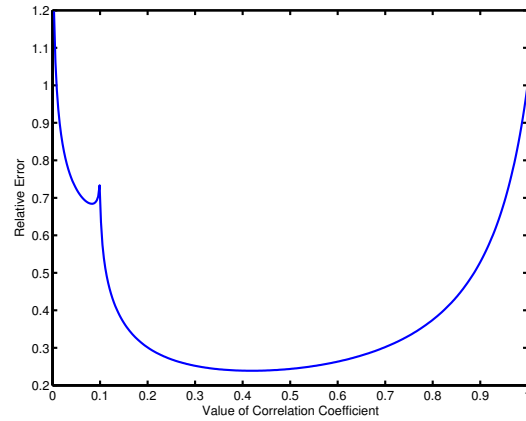


Fig. 6. Relative error in the estimate of K for a relative error of 10% in the correlation coefficients. The error is below 30% for coefficients between 0.2 and 0.7. The singularity observed at a correlation of 0.1 is due to the choice of a relative error of 10% or 0.1. This causes the logarithm in the numerator of (31) to approach infinity at that point.

e_K in the estimate of K for any correlation factor ρ' is given by:

$$e_K = \left| \frac{K - K'}{K} \right| = \left| \frac{\ln\left(\frac{\rho'}{e_{\rho'}}\right)}{\ln(\rho' - e_{\rho'})} \right|, \quad (31)$$

where $e_{\rho'}$ is the relative error in the correlation coefficient ρ' . The derivation is provided in the Appendix A.

Since it is not possible to determine the relative error in each correlation coefficient computed, $e_{\rho'}$ is assumed to be the same for all coefficients. Fig. 6 plots (31) for $e_{\rho'} = 0.1$ (i.e. 10%). It can be seen that the lowest relative errors in K are obtained for coefficients that lie within the 0.2 to 0.7 range. The reason for this becomes clear from a plot of the spatial correlation functions for various channel conditions (Fig. 7). The figure shows that the rate of change of the distance with respect to the correlation coefficient is the least over the 0.2 to 0.7 range – implying that a large uncertainty in the value of ρ leads to relative little error in the value of d , minimising the relative error in K . Therefore, L and M in (29) are chosen such that only coefficients with values within a certain range $[\rho_{\text{min}}, \rho_{\text{max}}]$ are considered.

Once an estimate of K is available, subsequent correlation coefficients ρ_k estimated at intervals of Δt , where $\Delta t \ll T_c$, can be used to obtain the associated set of distances d_k using (27). The corresponding set of speed estimates can then be obtained as follows:

$$v_{\text{est},k} = \frac{d_k}{k \times \Delta t}; \quad k = L, L + 1, \dots, M. \quad (32)$$

The final estimate is obtained by taking the arithmetic mean of the set of estimated speeds:

$$v_{\text{est}} = \frac{1}{M - L + 1} \sum_{k=L}^M v_{\text{est},k}. \quad (33)$$

For the algorithm to remain accurate and effective, the estimate of K must be periodically updated. Fig. 8 shows

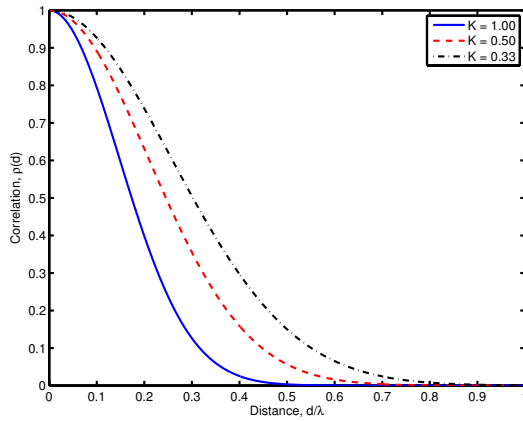


Fig. 7. Plot of the correlation function for various channel conditions. The gradient is steepest roughly between $\rho = 0.7$ and $\rho = 0.2$. Therefore, the rate of change of the distance with respect to the correlation coefficient is the lowest over that range. This implies that large errors in the value of ρ leads to relatively small errors in the estimate of d .

a flow chart of the algorithm.

IV. SIMULATION & RESULTS

MATLAB simulations are used to evaluate the performance of the speed estimation algorithms. The speed profile utilised is designed to emulate the motion of a pedestrian as illustrated by Fig. 9. The duration of the profile is 60s.

A. Method I: RRFSM

For simulation purposes, the RF signal source is assumed to be a DVB-T transmitter with a carrier frequency of 474MHz and OFDM symbols consisting of 1705 subcarriers (2K mode of DVB-T). The multipath channel is modeled as Rayleigh fading [8] with component phase offsets (ϕ_l) and time delays (τ_l) obtained from [10]. For simplicity, the AoAs (θ_l) are assumed to be time-invariant and uniformly distributed in $[0, 2\pi]$. Furthermore, it is also assumed that the channel response estimates are error free and displacement is in one dimension only. The correlation threshold is maintained at 0.95. The use of such a high threshold is justified since the CRE estimates are assumed to be perfectly known and error-free.

Fig. 10 shows the performance of the estimation algorithm at $d_a = 0.10m$ and $0.30m$. A moving average filter with a memory of 4ms is applied to the estimates for a smoother output. With $d_a = 0.10m$, a good match between the real and estimated speeds is obtained while a larger d_a shows relatively poorer performance. The reason for this becomes clear once the coherence time of the channel is taken into account. At a separation distance of $0.30m$, the time required by antenna B to traverse the inter-antenna separation distance is $0.6s$ for a constant speed of $0.5ms^{-1}$. However, at that speed, the coherence time of the channel is only about $0.54s$. Consequently,

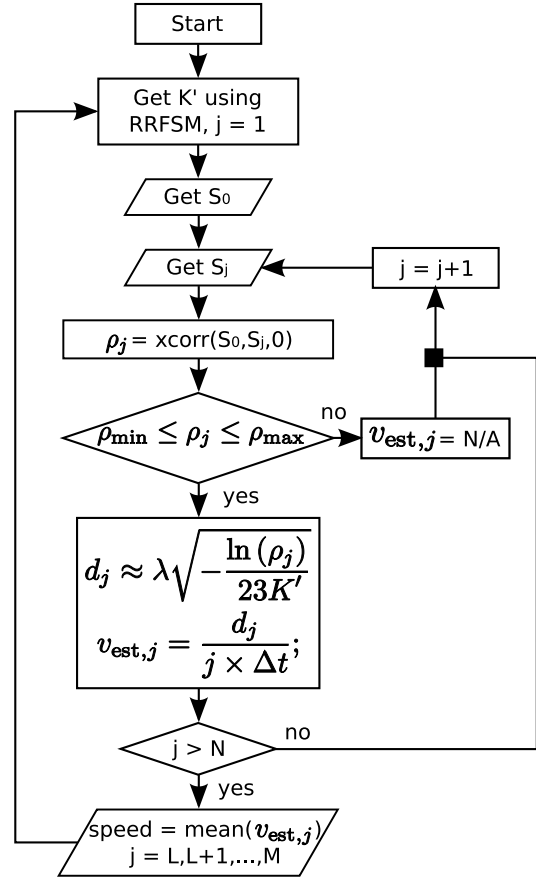


Fig. 8. Speed estimation algorithm utilising spatial correlation (modified RRFSM). S_j represents the j^{th} envelope. ρ_{min} and ρ_{max} define the coefficient range considered for speed estimation.

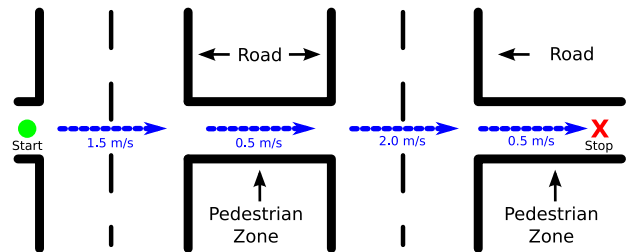


Fig. 9. Model of pedestrian behaviour. Starting from a standstill, the person crosses the street at an average speed of $1.5ms^{-1}$. On reaching the pavement on the other side, the speed reduces to a leisurely $0.5ms^{-1}$. When at the second road, the average speed increases to a brisk $2.0ms^{-1}$ for a fast crossing. Once on the other side, the speed returns to an average of $0.5ms^{-1}$ and is maintained till the pedestrian reaches the destination and stops.

the relevant CREs are no longer strongly correlated and a reliable speed estimate cannot be obtained.

The estimated profiles show that the algorithm tends to momentarily lose track of the speed when the device undergoes a sudden change in speed. This can be attributed to a radical change in the behaviour of the channel model. At constant speeds, the channel response is a function of linear time, t . However, when the device undergoes constant acceleration, the response becomes a function of the time squared, t^2 , as shown in the Appendix B. This implies that any CRE recorded at some time t_0 is in fact

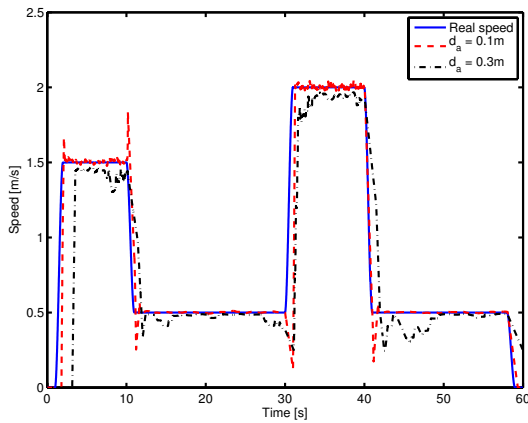


Fig. 10. Simulation of the relative RF signature matching algorithm for antenna separation distances (d_a) of 0.10m and 0.30m. The estimates are passed through a 4ms long moving average filter for smoothing. The speed profile used is the one illustrated in Fig. 9.

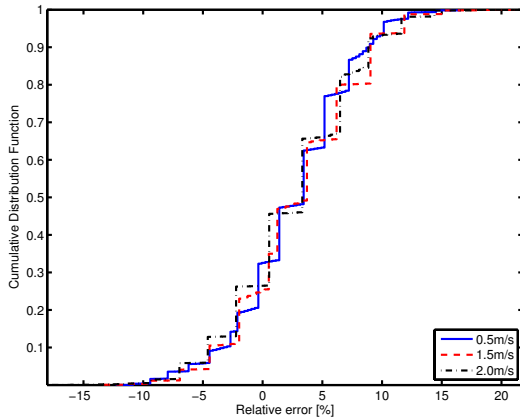


Fig. 11. CDF of relative errors in estimating speeds of 0.5ms^{-1} , 1.5ms^{-1} and 2.0ms^{-1} at an antenna separation distance of 0.10m. The time resolution issue described in section III-A manifests itself in the form of discrete steps in the error CDF.

similar to a CRE at time t_0^2 . This fundamental change in the recorded CREs leads to a disruption of algorithm and produces erroneous results at the points where there is a sudden change in the speed. Once the speed stabilises, however, the algorithm is quick to recover and continues tracking the real speed with a low error margin.

Fig. 11 shows cumulative distribution function (CDF) of the percentage errors ($\frac{v_{\text{est}} - v_{\text{real}}}{v_{\text{real}}} \times 100\%$) in estimating speeds of 0.5ms^{-1} , 1.5ms^{-1} and 2.0ms^{-1} at an antenna separation distance of 0.10m. From the plot it is evident that the performance of the algorithm is independent of the actual speed of the device. On average, the relative error is approximately 2.67% with a standard deviation of 5%. The quantisation of detectable speeds due to time resolution available (section III-A) also leads to discretisation of the relative error. This is the reason behind the stair-like CDF.

It may be noted that the average error is positive – indicating a tendency to overestimate the speed. Since

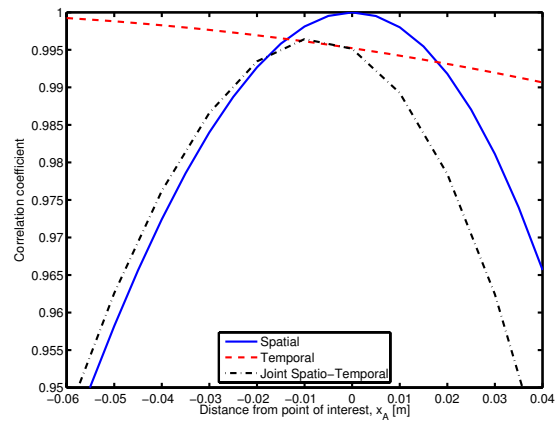


Fig. 12. Spatial and temporal correlation coefficients for a device with $d_a = 0.10\text{m}$ moving at 15ms^{-1} . As antenna B approaches the position previously occupied by antenna A (point of interest, x_A), the spatial correlation increases while the temporal correlation decreases. This leads to a joint maximum at a position shortly before x_A – leading to an underestimate of the time delay and hence an overestimate of the speed.

d_a is constant, this implies that the time delay is underestimated. This is due to the time-varying nature of the channel and a difference in the rate at which the spatial and temporal correlation functions evolve. Fig. 12 shows how the spatial and temporal correlation changes for a device with $d_a = 0.10\text{m}$ moving at 15ms^{-1} . Although a time axis, t , is not explicitly shown, it is related to the displacement axis, s , by the simple equation $t = \frac{s}{15} + c$, where c is some constant. It can be seen that as antenna B approaches the desired spatial location, x_A , the spatial correlation rapidly increases while the temporal correlation gradually decreases. As a result, the joint maximum of the correlation functions is not at the desired location but shortly before it – leading to an underestimate of the time delay and hence an overestimate of the speed.

B. Method II: Modified RRFSM

The simulator implemented is similar in design to the one described in Section IV-A.

Fig. 13 shows the performance of the modified RRFSM algorithm under different channel conditions as represented by the parameter K . It is assumed that perfect knowledge of the channel is available and hence the correlation coefficients ρ and the estimates of the parameter K are error free. From the plot, it is immediately clear that there is a near-perfect match between the real speed profile and that estimated by the algorithm – showing that the method described works as expected under ideal circumstances. The lack of any substantial difference between the estimates indicates that the results are not affected by the channel conditions. This is due to the assumption that both ρ and K are error free.

To investigate the impact of small uncertainties in the estimates of the parameter K , a uniformly distributed random relative error between $\pm 10\%$ is introduced. Fig.

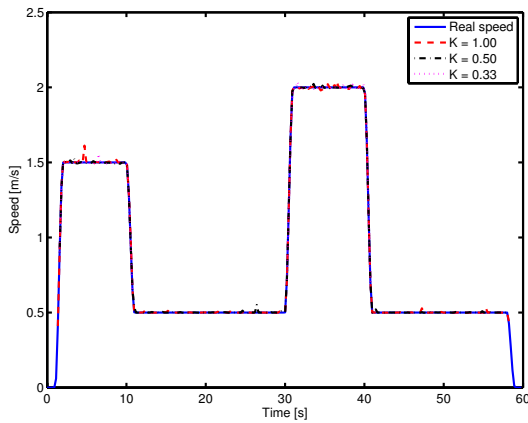


Fig. 13. Simulation of the spatial correlation algorithm for various channel conditions. Perfect knowledge of the channel parameters is assumed.

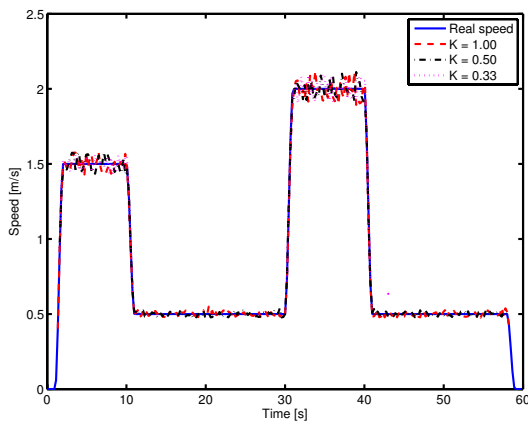


Fig. 14. Simulation of the spatial correlation algorithm for various channel conditions. The estimate of the parameter K is not exact and contains a random relative error uniformly distributed between $\pm 10\%$.

14 shows the results for different channel conditions as represented by the parameter K . As exact knowledge of the channel is no longer available, larger errors in the estimates appear. An analysis of the error statistics is provided later.

The plot reveals that no estimates are obtained for speeds that are below approximately 0.3ms^{-1} . A comparison of the minimum speeds detectable with the algorithm under various (exact) values of the parameter K is shown in Fig. 15. The general trend appears to be that the higher the value of K , the lower is the speed detectable. There are three contributing factors to this observation: the first is the relationship between ρ and K as described by (25), the second is related to the duration of each “run” of the algorithm and the third is tied to the choice of the “admissible” range of correlation coefficient values as shown in (29). The following attempts to explain the role each of these factors:

- 1) For a fixed value of d , (25) shows that $\rho \approx \exp[-XK]$ where X is a constant greater than

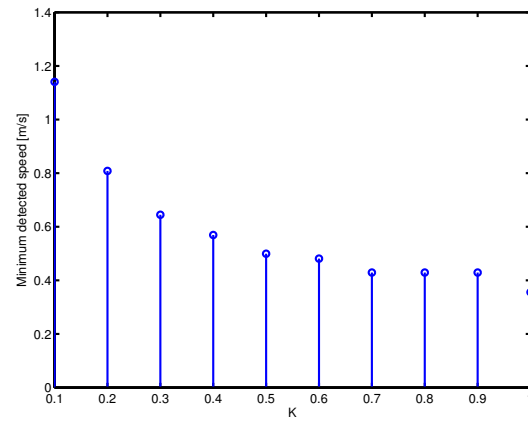


Fig. 15. Minimum speed detectable by the spatial correlation algorithm under various channel conditions for the speed profile shown in Fig. 13.

zero. This implies that the larger the value of K , the smaller the ρ for a given d .

- 2) At each run of the algorithm, the signal envelope is estimated at intervals of Δt seconds for a total duration of T seconds where T is predetermined and fixed. At low speeds, a relatively small distance is travelled by the device in T seconds and as a result, the channel still remains highly correlated after that run.
- 3) As explained in Section III-B, only those values of ρ that fall within a certain range are utilised for speed estimation. Values that are too high or too low are ignored to minimise errors.

The consequence of the above is that at low speeds, the correlation coefficient for smaller values of K is higher than the upper bound defined and hence no estimate can be obtained. For the same speed, (25) implies that a larger K may perform better as it leads to a lower value of ρ . If that value is lower than the upper bound to admissible correlation coefficients, an estimate of the speed can be obtained. Since the minimum detectable speed clearly depends on a number of user-set parameters, it may be possible to lower the bound by increasing the time between runs and relaxing the $[\rho_{\min}, \rho_{\max}]$ limits placed on the correlation coefficients considered for speed estimation.

To investigate the error performance of the algorithm, simulations are performed at typical pedestrian speeds of 1.0ms^{-1} , 1.5ms^{-1} and 2.0ms^{-1} . The percentage relative error in the estimates (where available) are computed using $\frac{v_{\text{est}} - v_{\text{real}}}{v_{\text{real}}} \times 100\%$. When the channel parameters are known exactly, the mean error in the estimates is less than 0.04% with a standard deviation of approximately 0.86% .

Fig. 16 shows the CDF of the errors when the estimate of the parameter K contains a random relative error uniformly distributed between $\pm 10\%$. As the error CDFs are very similar to one another, it is reasonable to conclude that the relative error in the estimates is independent of

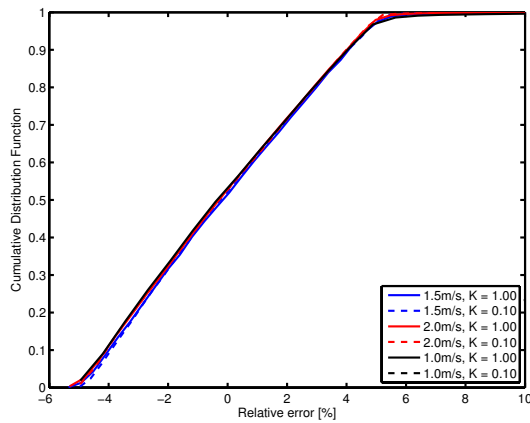


Fig. 16. CDF of relative errors in estimating speeds of 1.0ms^{-1} , 1.5ms^{-1} and 2.0ms^{-1} . The estimate of the parameter K has a random relative error uniformly distributed between $\pm 10\%$.

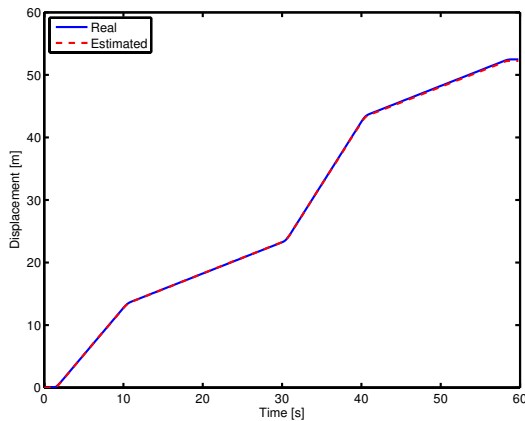


Fig. 17. Displacement (real and estimation) of a device moving according to Fig. 9 using the modified RRFSM algorithm with a 10% uncertainty in the parameter K . Despite the errors in K , the estimate is still excellent (error of 24.5cm after 60s) due to the fact that overestimates and underestimates in the speed cancel each other (as seen in Fig. 14).

both the speed and the actual channel characteristics. With a 10% uncertainty in the parameter K , the average error in the estimates is less than 0.15% with a standard deviation of approximately 3%.

Fig. 17 shows how the estimate of the displacement is affected by the errors in the speed estimates for a device moving according to the model in Fig. 9. After 60s, the error in displacement estimate is a mere 24.5cm. The error in the estimate is very low due to the fact that overestimates and underestimates in the speed cancel each other – resulting in a mean error that is very close to zero. This is particularly beneficial in context of PDR where the accumulation of error is a common problem.

To summarise, the basic RRFSM algorithm provides good results (2.67% error around pedestrian speeds on average) with a relatively low complexity. The modified RRFSM scheme requires additional computations but produce excellent speed estimates (0.15% error on average)

even when accurate estimates of the model parameters are unavailable.

V. SUMMARY AND CONCLUSION

The spatial correlation properties of a multipath fading channel are exploited for speed estimation. If, in addition, heading information is available through an electronic compass, for example, indoor pedestrian dead reckoning can be performed. This enables the determination of the position of a mobile device, and hence, allows mobile navigation at places where GPS fails to work.

First, it is demonstrated that the RRFSM algorithm based on two antennas separated by a known distance provides speed estimation errors of less than 2.67% on average at typical pedestrian velocities. A by-product of this algorithm is a metric that characterises the actual propagation environment which, in turn, helps establish an environment specific relationship between the spatial correlation coefficient and the antenna displacement. This relationship is exploited by a modified RRFSM algorithm, with a further improvement of the accuracy (relative error of 0.15% or less on average even when the propagation environment cannot be estimated exactly) at the cost of a slightly increased computational complexity. Both algorithms can be combined intelligently to provide the best estimates possible. Where applicable, the modified RRFSM algorithm can be utilised to improve the speed estimate. Otherwise, the basic RRFSM algorithm is used as a fall-back solution since it generally also provides good estimates.

Simulations also show that when the modified RRFSM method is used for speed and subsequently displacement estimation, the error accumulated is very low. After 60s, the estimate differs by only 24.5cm for a typical pedestrian speed profile. This indicates that the algorithm is ideal for use in PDR applications where a high rate of accumulation of error is a common problem.

As no assumptions are made about the environment, the schemes are completely self-sufficient. The only requirement is a source of RF signal that leads to a fading channel at the receiver. Since the methods do not rely on the properties of any particular wireless standard, any wideband system capable of effectively capturing the effect of a fading channel is usable. In this paper, DVB-T is chosen for its wideband nature (8MHz channels) and ubiquity.

With the recent influx of MIMO capable devices, the low computational complexity of the proposed algorithms and the fact that some of the required information such as the channel estimates is simply recycled from the data detection process, the speed estimation algorithms can easily be integrated into current mobile communication devices.

At this point, one of the largest open issues is the extension of the algorithms to multiple dimensions. As mentioned earlier in Section III-A, this can be achieved with at least two antennae in each of the spatial dimensions desired. Preliminary investigations with multi-

antenna arrays have produced promising results but require further research. The multi-antenna array is also useful for heading estimation – opening up the possibility of “one-step” location estimates using the proposed basic algorithms.

Other issues that merit further research are assessment and mitigation of errors due to acceleration, investigations of the robustness of the algorithms under real-world conditions and the development of a mechanism for the determination of the level of accuracy in any estimate of the channel dependent parameter K .

APPENDIX A

DERIVATION OF THE RELATIVE ERROR IN K

Given a correlation coefficient ρ' and the associated distance d' , an estimate K' can be obtained using (28):

$$\begin{aligned} K' &= -\frac{\ln(\rho')}{23} \left(\frac{\lambda}{d'}\right)^2 \\ &= C \frac{\ln(\rho')}{(d')^2}, \end{aligned} \quad (34)$$

where C is a constant. Assuming that the real value of the coefficient is ρ , the true K is then:

$$\begin{aligned} K &= -\frac{\ln(\rho)}{23} \left(\frac{\lambda}{d'}\right)^2 \\ &= C \frac{\ln(\rho' - e_{\rho'})}{(d')^2}, \end{aligned} \quad (35)$$

where $e_{\rho'}$ is the relative error in the correlation coefficient.

Therefore, the error in the estimate for K is given by:

$$\begin{aligned} K' - K &= C \frac{\ln(\rho')}{(d')^2} - C \frac{\ln(\rho' - e_{\rho'})}{(d')^2} \\ &= C \frac{\ln\left(\frac{\rho'}{\rho' - e_{\rho'}}\right)}{(d')^2}. \end{aligned} \quad (36)$$

Rewriting (27) as

$$\begin{aligned} (d')^2 &= \frac{\lambda^2}{-23} \times \frac{\ln(\rho)}{K} \\ &= C \frac{\ln(\rho' - e_{\rho'})}{K} \end{aligned} \quad (37)$$

and substituting into (36), an expression for the relative error in K , e_K , is obtained:

$$e_K = \left| \frac{K - K'}{K} \right| = \left| \frac{\ln\left(\frac{\rho'}{\rho' - e_{\rho'}}\right)}{\ln(\rho' - e_{\rho'})} \right|. \quad (38)$$

APPENDIX B

ACCELERATION AND CHANNEL RESPONSE

For a receiver with a single antenna, the spatio-temporal transfer function, $H(t, f, x)$, with time invariant multipath components can be written as

$$H(t, f, x) = \sum_{l=0}^{L-1} A_l e^{j2\pi f d(l)t + j\phi_l - j2\pi \tau_l f} a(\theta_l) \quad (39)$$

where $f_{d(l)}$ is the Doppler spread associated with the component l and all other parameters are as previously defined in Section II. Substituting the one-dimensional version of (2) into (39) and rewriting the Doppler spread as a function of the speed v and angle ω_l ,

$$\begin{aligned} H(t, f, x) &= \sum_{l=0}^{L-1} A_l \exp \left[j2\pi \frac{v}{\lambda} \cos(\omega_l) t \right. \\ &\quad \left. + j\phi_l - j2\pi \tau_l f - \beta \cos(\theta_l) x \right]. \end{aligned} \quad (40)$$

Since $v = v_0 + bt$ and $x = x_0 + v_0 t + \frac{1}{2}bt^2$, where v_0 is the initial speed, x_0 is the initial position and b is the constant acceleration,

$$\begin{aligned} H(t, f, x) &= \sum_{l=0}^{L-1} A_l \exp \left[j2\pi \frac{v_0 + bt}{\lambda} \cos(\omega_l) t \right. \\ &\quad \left. + j\phi_l - j2\pi \tau_l f \right. \\ &\quad \left. - \beta \cos(\theta_l) \left(x_0 + v_0 t + \frac{1}{2}bt^2 \right) \right]. \end{aligned} \quad (41)$$

From (41) it is clear that the response is non-linear in t when the acceleration is non-zero.

REFERENCES

- [1] J. Collin, O. Mezentsev, and G. Lachapelle, “Indoor Positioning System Using Accelerometry and High Accuracy Heading Sensors,” in *Proc. of ION GPS/GNSS 2003 Conference*. Portland, OR: Institute of Navigation, Sep. 9–12, 2003.
- [2] J. Kappi, J. Syrjarinne, and J. Saarinen, “MEMS-IMU Based Pedestrian Navigator for Handheld Devices,” in *Proc. of ION GPS 2001 Conference*. Salt Lake City, UT: Institute of Navigation, Sep. 11–14, 2001, pp. 1369 – 1373.
- [3] C. Randell, C. Djalllis, and H. Muller, “Personal Position Measurement Using Dead Reckoning,” *Proceedings of the 7th IEEE International Symposium on Wearable Computers 2003*, pp. 166–173, Oct.18–21, 2005.
- [4] A. Abdi and M. Kaveh, “Level Crossing Rate in Terms of the Characteristic Function: a New Approach for Calculating the Fading Rate in Diversity Systems,” *IEEE Transactions on Communications*, vol. 50, no. 9, pp. 1397–1400, Sep. 2002.
- [5] L. Zhao and J. W. Mark, “Mobile Speed Estimation Based on Average Fade Slope Duration,” *IEEE Transactions on Communications*, vol. 52, no. 12, pp. 2066–2069, Dec. 2004.
- [6] R. Narasimhan and D. C. Cox, “Speed Estimation in Wireless Systems Using Wavelets,” *IEEE Transactions on Communications*, vol. 47, no. 9, pp. 1357–1364, Sep. 1999.
- [7] R. B. Ertel, P. Cardieri, K. W. Sowerby, T. S. Rappaport, and J. H. Reed, “Overview of Spatial Channel Models for Antenna Array Communication Systems,” *IEEE Personal Communications [see also IEEE Wireless Communications]*, vol. 5, no. 1, pp. 10–22, Feb. 1998.
- [8] P. Höher, “A Statistical Discrete-Time Model for the WSSUS Multipath Channel,” *IEEE Transactions on Vehicular Technology*, vol. 41, no. 4, pp. 461–468, Nov. 1992.
- [9] T. S. Rappaport, *Wireless Communications: Principles and Practice*, 2nd ed. Prentice Hall PTR, Dec. 2001.
- [10] ETSI EN 300 744 v1.5.1 (2004-06), *Digital Video Broadcasting (DVB); Framing Structure, Channel Coding and Modulation for Digital Terrestrial Television*, European Telecommunications Standards Institute (ETSI) Std., Jun. 2004.
- [11] G. Durgin and T. Rappaport, “Theory of Multipath Shape Factors for Small-Scale Fading Wireless Channels,” *IEEE Transactions on Antennas and Propagation*, vol. 48, no. 5, pp. 682–693, 2000.
- [12] M. Afgani and H. Haas, “Speed Estimation Using Relative Radio Frequency Signature Matching,” in *Proc. of the 66th IEEE Vehicular Technology Conference (VTC)*, Baltimore, USA, Oct. 1–3, 2007, pp. 1970–1974.

- [13] S. Beauregard and H. Haas, "Pedestrian Dead Reckoning (PDR) and GPS for Indoor Positioning," in *Proc. of 3rd Workshop on Positioning, Navigation and Communication (WPNC)*, Hannover, Germany, Mar. 16, 2006.

Mostafa Afgani received his B.Sc. in Electrical Engineering and Computer Science (2004) and M.Sc. in Electrical Engineering (2006) from Jacobs University Bremen, Germany. He is currently working towards his PhD degree at the Institute for Digital Communications (IDCOM) in the University of Edinburgh.

Sinan Sinanović has obtained his Ph.D. in electrical and computer engineering from Rice University, Houston, Texas in 2006. In the same year, he has joined Jacobs University Bremen in Germany as a post doctoral fellow. In 2007, he has joined the University of Edinburgh in the UK where he currently works as a research fellow in the Institute for Digital Communications. He has previously worked for Texas Instruments in Dallas, Texas on ASIC for the central office modem. While working for Halliburton Energy Services in Houston, Texas, he developed acoustic telemetry receiver for which he was awarded US patent (# 7158446). He is a member of the Tau Beta Pi engineering honour society and a member of Eta Kappa Nu electrical engineering honour society. He earned his M.S. from Rice University and his B.S.E.E. (summa cum laude) from Lamar University in Texas. He won national mathematics contest in Bosnia and was awarded honourable mention at the International Mathematics Olympiad in Hong Kong, both in 1994.

Karim Khashaba received his B.Sc. in Electrical Engineering and Computer Science in 2007 from Jacobs University Bremen. He is currently working towards his M.Sc. in Communication Systems at the Technical University Munich.

Harald Haas received the PhD degree from the University of Edinburgh in 2001. His main research interests are in the areas of wireless system engineering and digital signal processing, with a particular focus on interference aware MAC protocols, multiuser access, link adaptation, scheduling, dynamic resource allocation, multiple antenna systems and optical wireless communication. From 2001 to 2002, Dr. Haas was project manager at Siemens AG (Information and Communication Mobile Networks) for an international research project on new radio access technologies. Dr. Haas joined International University Bremen (Germany), now Jacobs University Bremen, in September 2002 where he has since been Associate Professor of Electrical Engineering. In June 2007, Dr. Haas joined the University of Edinburgh (Scotland/UK) where he is Reader in the Institute for Digital Communications (IDCOM). Dr. Haas received a best paper award at the International Symposium on Personal, Indoor and Mobile Radio Communications (PIMRC) in Osaka/Japan in 1999 and holds more than 12 patents in the area of wireless communications. Dr. Haas contributed a chapter to the "Handbook of Information Security" entitled "Air Interface Requirements for Mobile Data Services" by John Wiley & Sons, Inc. He co-authors a book entitled "Next Generation Mobile Access Technologies: Implementing TDD" with Cambridge University Press. His work on optical wireless communication was selected by a jury of renowned scientists installed by the German ministry of education and research (BMBF) for publication in "100 Produkte der Zukunft (100 Products of the Future)" authored by Nobel Laureate T. W. Hänsch.